On the Link Layer Performance of Narrowband Body Area Networks

J.-M. Dricot[1], G. Ferrari[2], S. Van Roy[1], Fr. Horlin[1], and Ph. De Doncker[1]

1. Université Libre de Bruxelles
OPERA – Wireless Communications Group
E-mail: {jdricot, svroy, fhorlin, pdedonck}@ulb.ac.be

2. University of Parma, Italy
Dept. of Information Engineering
E-mail: gianluigi.ferrari@unipr.it

***Abstract*—Personal area networks and, more specifically, body area networks (BANs) are key building blocks of the future generation networks and the Internet of Things as well. In the last years, research has focused on the channel modeling and the definition of efficient medium access control (MAC) mechanisms. Less attention was paid to network-level performance. Thereby, this paper presents a novel analytical model for network performance analysis with centralized and mesh topologies. This model takes into account the channel statistics (i.e., the large-scale fading) and delivers several insights on the BAN implementation.**

I. Introduction

Recent advances in ultra-low power sensors have fostered the research in the field of body-centric networks, also referred to as *body area networks* (BANs). In these networks, a set of nodes (called *sensors*) is deployed on the human body. They aim at monitoring and reporting several physiological values, such as blood pressure, breath rate, skin temperature, or heart beating rate. A pictoral example of a BAN is shown in Fig. 1, where two illustrative topologies are presented: (i) a centralized topology, where a special node (denoted as "HUB") acts as a sink for all communications initiated by the sensor and (ii) a mesh topology (or "multi-hop topology"), where several intermediary nodes relay the information from the source node to the destination (e.g., when data fusion or sensor cooperation is required).

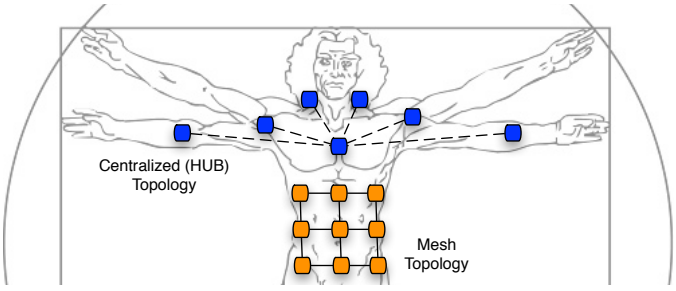

Fig. 1: Body Area Network.

Most of the time, sensing is performed at low rates but, in case of emergency, the network load may increase in seconds. Therefore, an in-depth analysis of the network outage, throughput, and achievable transmission rate can give insights on the maximum supported reporting rate and the corresponding performance.

The focus of this paper is on multi-hop communications and the impact of the specificities of the propagation channel. The modeling of the BAN channel has recently been thoroughly investigated [1]–[5]. The main findings on the body radio propagation channel can be summarized as follows. First, the average value of the power decreases as an exponential function of the distance. However, unlike classical propagation models, where the received power P is a decreasing function of the distance of the form $d^{-\alpha}$, in [6] the authors prove that a law of the form $10^{-\gamma d}$ characterizes more accurately body radio propagation. Second, the propagation channel is subject to large-scale fading (that is, shadowing). This variation follows a zero-mean Gaussian distribution in the dB scale or a Log-normal distribution in the linear scale.

This paper addresses the evaluation of the *throughput* for BANs, being this metric a traditional measure of how much traffic can be delivered by the network [7], [8]. Therefore, our analysis is expedient to understand the level of information which could be collected and processed in body-related applications (e.g., health or fitness monitoring). We consider slotted and asynchronous communications such that, in every time slot, each node transmits independently with a probability p. Indeed, in a generic scenario, the traffic distribution in a sensor network can be considered as spatially and temporally bursty, that is, reporting periods alternate temporally and spatially with periods and areas with little or no traffic (or even with a scheduled sleep of the nodes). It may therefore be impractical to employ reservation-based MAC schemes, such as those based on time/frequency division multiple access (TDMA/FDMA), that require a substantial amount of coordination traffic and cannot be implemented efficiently in energy- and computation-constrained sensor nodes.

The rest of the paper is organized as follows. In Section II, the models, definitions, and notations are introduced. Then, in Section III, the conditional success probability of a transmission for a node given the transmitter-receiver and interference-receiver distances is derived. Section IV investigates the average link throughput and achievable transmission rate for centralized and mesh topologies. Section V concludes the paper.

This work is supported by the Belgian National Fund for Scientific Research (FRS-FNRS).
Corresponding author: Jean-Michel Dricot (jdricot@ulb.ac.be)

II. Models, notation, and definitions

A. Stochastic Channel Model

Defining as $P_i^{(\mathrm{r})}$ the received power from the i-th node at distance d gives

$$P_i(d) = P_i \; L(d_i)\mathbf{X}_i$$

where P_i is the emitted power, $L(d)$ is the loss at distance d, it accounts for the antenna gains and carrier frequency, and $\mathbf{X}_i$ is a random variable (RV) which depends on the channel characteristics. It is shown in [9] that $\mathbf{X}_i$ has a log-normal distribution[1] with parameters μ and σ, i.e., its cumulative distribution function (cdf) is

$$F_{\mathbf{X}_i}(x;\mu,\sigma) = \frac{1}{2} - \frac{1}{2}\mathrm{erf}\left(\frac{\mu_{\mathrm{dB}} - 10\log_{10} x}{\sigma_{\mathrm{dB}}\sqrt{2}}\right)$$

where σ_{dB} typically ranges from 4 dB to 10 dB, μ_{dB} is the average path loss on the link (dimension: [dB]). Since the loss is accounted for by the term $L(d)$, it follows that $\mu_{\mathrm{dB}} = 0$ and the cdf of $\mathbf{X}_i$ reduces to the following:

$$F_{\mathbf{X}_i}(x;0,\sigma) = \frac{1}{2} - \frac{1}{2}\mathrm{erf}\left(\frac{-10\log_{10} x}{\sigma\sqrt{2}}\right)$$

and its corresponding pdf is

$$f_{\mathbf{X}_i}(x;0,\sigma) = \frac{10}{(\ln 10)\; x\; \sqrt{2\pi}\sigma}\exp\left\{-\frac{(10\log_{10} x)^2}{2\sigma^2}\right\}. \quad (1)$$

In [6], [10], it is shown, on the basis of an extensive campaign of measurements, that the path loss (in dB scale) is a linearly increasing function of the distance, i.e.:

$$P_i - P_i(d_i) = L_{\mathrm{ref}} + 10\gamma(d_i - d_{\mathrm{ref}}) \qquad d_i > d_{\mathrm{ref}}$$

where d_{ref} is a reference distance, L_{ref} is the loss at that distance, and γ a suitable constant. For instance, in [10] the authors found $d_{\mathrm{ref}} = 8$ cm, $L_{\mathrm{ref}} = 55.18$ dB, and $\gamma = 1.26$dB/cm. The path loss, in linear scale, can then be expressed as follows:

$$\begin{aligned} L(d_i) &= 10^{(10\gamma d_{\mathrm{ref}} - L_{\mathrm{ref}})/10}.10^{-\gamma d_i} \\ &\triangleq L_0\, 10^{-\gamma d_i}. \end{aligned} \quad (2)$$

B. Traffic Model

The transmission state of the i-th node at time[2] t is represented by the following RV:

$$\mathbf{\Lambda}_i(t) = \begin{cases} 1 & \text{if the } i\text{-th node transmits at time } t \\ 0 & \text{if the } i\text{-th node is silent at time } t. \end{cases}$$

A simple random access scheme is such that, at each time slot, a node transmits with probability p [11, p. 278]. Therefore, $\{\mathbf{\Lambda}_i(t)\}_{t=1}^{\infty}$ is a sequence of Bernoulli RVs with $\forall t$: $\mathbb{P}\{\Lambda_i(t) = 1\} = p$.

[1]Note that we use the $\log_{10}$ variant of the log-normal since the widely-used shadowing model uses an additive Gaussian variation expressed in dB.

[2]For the sake of simplicity, we assume that t can take integer values, i.e., we refer to a slotted communication system.

C. Total Interference Power

A transmission in a given link is successful if and only if the signal-to-noise and interference ratio (SINR) is above a certain threshold θ. This threshold value depends on the receiver characteristics, the modulation format, and the coding scheme, among others. The SINR at the receiving node of the link is given by

$$\mathrm{SINR} \triangleq \frac{P_0(d_0)}{W + P_{\mathrm{int}}} \quad (3)$$

where $P_0(d_0)$ is the received power from the link source located at distance d_0, W is ambient the noise power, and P_{int} is the total interference power at the link receiver, that is, the sum of the received power from all the undesired transmitters:

$$P_{\mathrm{int}} \triangleq W + \sum_{i=1}^{N} P_i(d_i)\; \mathbf{\Lambda}_i = W + \sum_{i=1}^{N} P_i L(d_i)\; \mathbf{X}_i\mathbf{\Lambda}_i.$$

D. Link Throughput and Link Transport Capacity

A *transmission is successful* if the channel is not in an outage, i.e., if the (instantaneous) SINR exceeds a certain threshold θ, that is, $\mathcal{P}_{\mathrm{s}} = \mathbb{P}\{\mathrm{SINR} > \theta\}$.

The *probabilistic link throughput* (adimensional) is defined to be the success probability multiplied by the probability that the transmitter actually transmits (in full-duplex operation) and, in addition in half-duplex operation, the receiver actually listens. So it is the unconditioned reception probability. This is the throughput achievable with a simple ARQ scheme (with error-free feedback) [12]. For the slotted transmission scheme we consider, the half-duplex probabilistic throughput is $\tau^{\mathrm{half}} \triangleq p(1-p)\mathcal{P}_{\mathrm{s}}$ and for full-duplex it is $\tau^{\mathrm{full}} \triangleq p\,\mathcal{P}_{\mathrm{s}}$.

Finally, the *link achievable transmission rate* (dimension: [bit/s/Hz]) is defined as the product of the probabilistic throughput and the link capacity, i.e., $T = \tau\, \log_2(1 + \mathrm{SINR})$.

III. Success Probability of a Transmission

A. Derivation

The link probability of success for a required threshold SINR value equal to θ is

$$\begin{aligned} \mathcal{P}_{\mathrm{s}} &= \mathbb{P}\{\mathrm{SINR} > \theta\} \\ &= \mathbb{E}\left[\mathbb{P}\left\{\frac{P_0\; L(d_0)\mathbf{X}_0}{P_{\mathrm{int}}} > \theta \;\middle|\; P_{\mathrm{int}}\right\}\right] \\ &= \mathbb{E}_{X,\lambda}\left[1 - \mathbb{P}\left\{\mathbf{X}_0 \le \theta\frac{W + \sum_{i=1}^{N} P_i\, L(d_i)\mathbf{X}_i\mathbf{\Lambda}_i}{P_0\, L(d_0)}\right\}\right] \\ &= \mathbb{E}_{X,\lambda}\left[\frac{1}{2} + \frac{1}{2}\mathrm{erf}\left(\frac{-10\log_{10}\theta\boldsymbol{\eta}}{\sigma\sqrt{2}}\right)\right] \end{aligned} \quad (4)$$

where

$$\boldsymbol{\eta} \triangleq \frac{W + \sum_{i=1}^{N} P_i\, L(d_i)\mathbf{X}_i\mathbf{\Lambda}_i}{P_0\, L(d_0)} = \frac{W}{P_0\, L(d_0)} + \sum_{i=1}^{N}\eta_i\mathbf{X}_i\mathbf{\Lambda}_i. \quad (5)$$

In the Appendix, it is shown that

$$\zeta(z;\sigma) = \frac{1}{2} + \frac{1}{2}\mathrm{erf}\left(\frac{-10\log_{10} z}{\sigma\sqrt{2}}\right) \approx \sum_{j}^{n} c_j \exp(-a_j z)$$

$$\mathcal{P}_{\mathrm{s}} = \sum_{j=1}^{n} c_j \underbrace{\exp\left(\frac{-a_j \theta W}{P_0\, L_0\, 10^{-\gamma d_0}}\right)}_{\text{Background noise}} \prod_{i=1}^{N} \left[p \underbrace{\int_0^{\infty} \exp\left(-a_j \theta \frac{P_i}{P_0}\, 10^{\gamma(d_0-d_i)} x_i\right) f_{\mathbf{X}}(x_i)\, \mathrm{d}x_i}_{\text{Interference}} + (1-p) \right] \tag{6}$$

where $\{c_j\}_{j=1\ldots n}$, $\{-a_j\}_{j=1\ldots n}$ are suitable coefficients, so that

$$\begin{aligned}\zeta(\theta\boldsymbol{\eta}) &= \sum_{j=1}^{n} c_j \exp\left(\frac{-a_j\theta W}{P_0\, L(d_0)}\right) \exp\left(-a_j\, \theta \sum_{i=1}^{N} \eta_i \mathbf{X}_i \boldsymbol{\Lambda}_i\right) \\ &= \sum_{j=1}^{n} \underbrace{c_j \exp\left(\frac{-a_j\theta W}{P_0\, L(d_0)}\right)}_{c'_j} \prod_{i=1}^{N} \exp\left(-a_j \theta \eta_i \mathbf{X}_i \boldsymbol{\Lambda}_i\right)\end{aligned}$$

and

$$\begin{aligned}\mathbb{E}_X\left[\frac{1}{2} + \frac{1}{2}\mathrm{erf}\left(\frac{-10\log_{10}\theta\boldsymbol{\eta}}{\sigma\sqrt{2}}\right)\right] &= \mathbb{E}_X\left[\zeta(\theta\boldsymbol{\eta})\right] \\ &= \underbrace{\int_0^{\infty} \ldots \int_0^{\infty} \int_0^{\infty}}_{N \text{ times}} \zeta(\theta\boldsymbol{\eta}) \times \prod_{i=1}^{N} f_{\mathbf{X}}(x_i)\, \mathrm{d}x_i \\ &= \sum_{j=1}^{n} c'_j \prod_{i=1}^{N} \int_0^{\infty} \exp\left(-a_j \theta \eta_i x_i \boldsymbol{\Lambda}_i\right) f_{\mathbf{X}}(x_i)\, \mathrm{d}x_i\end{aligned}$$

Finally, (4) becomes

$$\begin{aligned}&\mathcal{P}_{\mathrm{s}} = \mathbb{E}_{\Lambda}\, \mathbb{E}_X\left[\zeta(\theta\boldsymbol{\eta})\right] \\ &= \mathbb{E}_{\Lambda}\left[\sum_{j=1}^{n} c'_j \prod_{i=1}^{N} \int_0^{\infty} \exp\left(-a_j\theta\eta_i x_i \boldsymbol{\Lambda}_i\right) f_{\mathbf{X}}(x_i)\, \mathrm{d}x_i\right] \\ &= \sum_{j=1}^{n} c'_j \prod_{i=1}^{N} \mathbb{E}_{\Lambda}\left[\int_0^{\infty} \exp\left(-a_j\theta\eta_i x_i \boldsymbol{\Lambda}_i\right) f_{\mathbf{X}}(x_i)\, \mathrm{d}x_i\right] \\ &= \sum_{j=1}^{n} c'_j \prod_{i=1}^{N} \left[\mathbb{P}\left\{\lambda_i = 1\right\} \int_0^{\infty} \exp\left(-a_j\theta\eta_i x_i\right) f_{\mathbf{X}}(x_i)\, \mathrm{d}x_i \right. \\ &\qquad \left. + \mathbb{P}\left\{\lambda_i = 0\right\} \int_0^{\infty} f_{\mathbf{X}}(x_i)\, \mathrm{d}x_i\right] \\ &= (6)\end{aligned}$$

which can be numerically computed.

B. Narrowband Communications

The first term of (6) defines the link probability of success in a noise-limited regime, i.e., even if no interferers are present. Starting from (4) with $P_{\mathrm{int}} = 0$ gives:

$$\mathcal{P}_{\mathrm{s}} = \zeta\left(\frac{\theta W}{P_0\, L_0\, 10^{-\gamma d_0}}\right).$$

If a threshold link probability of success equal to $\mathcal{P}_{\mathrm{s}}^{\mathrm{th}}$ is required and W is the thermal noise, a transmission is possible if and only if

$$P_0 \geq \frac{\theta\, kTB}{L_0\, \zeta^{-1}(\mathcal{P}_{\mathrm{s}}^{\mathrm{th}})}\, 10^{\gamma d_0} \qquad 0 < \mathcal{P}_{\mathrm{s}}^{\mathrm{th}} < 1 \tag{7}$$

where $T = 300$ K is the room temperature, k is the Boltzmann's constant, and B is the transmission bandwidth. For instance, in Fig. 2 the minimum transmission power P_0 for a ZigBee equipment ($B = 5$ MHz), operating at $T = 30°$C with a SINR $\theta = 10$ dB and $\sigma = 4$ dB, is shown as a function of the distance, considering various values of the required link probability of success of $\mathcal{P}_{\mathrm{s}}^{\mathrm{th}}$.

It can be seen that (i) the value of $\mathcal{P}_{\mathrm{s}}^{\mathrm{th}}$ plays a limited role on the transmission power[3] and (ii) if the transmission power is constrained by energy concerns, only short-range communications (some tenths of centimeters) will be possible. A *multi-hop* network architecture is therefore preferred.

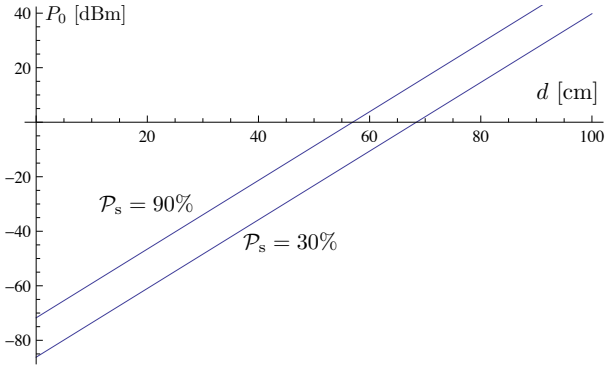

Fig. 2: Minimum transmission power as a function of the distance.

In the following, we will consider only interfence-limited networks, i.e., scenarios where condition (7) is satisfied. Formally, this situation is equivalent to letting $W = 0$ in (6).

IV. Performance Analysis

In this section, we investigate networks with two topologies: (i) a centralized (hub) architecture in which all nodes connect to a central sink and (ii) a mesh architecture where every node has the same number of nearest neighbors and the same distance to all nearest neighbors. Without any loss of generality, we assume that all nodes are equivalent and, therefore, transmit at equal power levels, i.e., $\forall i, j \in \{0, N\} : P_i = P_j$.

A. Hub Topologies

Fig. 3 presents a centralized architecture, where a central node (called *hub* or *sink*) is surrounded by several nodes. These nodes can be leaves of the routing tree or, in a star topology, the coordinators of each star. In this architecture, all distances between the nodes and the hub are approximately the same

[3] Indeed, $\forall x \in \mathbb{R} : |x| < 1 \Rightarrow |\,\mathrm{erf}(x)| \leq 2$. Therefore, since $10\log_{10}\zeta_{\mathrm{dB}}^{-1}(x) = -\sigma\sqrt{2}\,\mathrm{erf}^{-1}(2x-1)$, one has $|10\log_{10}\zeta_{\mathrm{dB}}^{-1}(x)| \leq 2\sigma\sqrt{2}$. For instance, with $\sigma = 4$ dBm, this bound is $2\sigma\sqrt{2} = 11.3$ dBm.

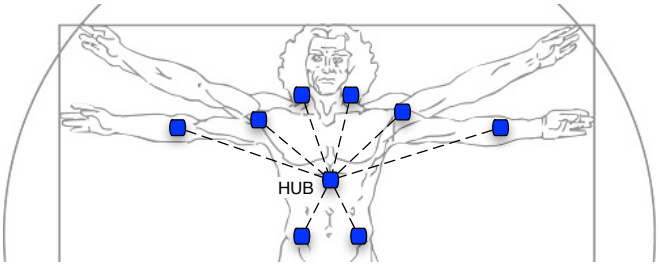

Fig. 3: Central hub surrounded by several nodes.

(i.e., $\forall i \in \{1,\dots,N\} : d_i \approx d_0$) and the link probability of success at the hub becomes

$$\mathcal{P}_{\mathrm{s}} = N \sum_{j=1}^{n} c_j \left[p \int_0^{\infty} \exp\left(-a_j \theta x_i\right) f_{\mathbf{X}}(x_i)\, \mathrm{d}x_i + (1-p) \right].$$

The link achievable transmission rate is shown in Fig. 4 for full- and half-duplex systems. It can be seen that both transmission strategies exhibit same performance when (i) the number of nodes N to serve increases and (ii) the data collection (through p) remains limited.

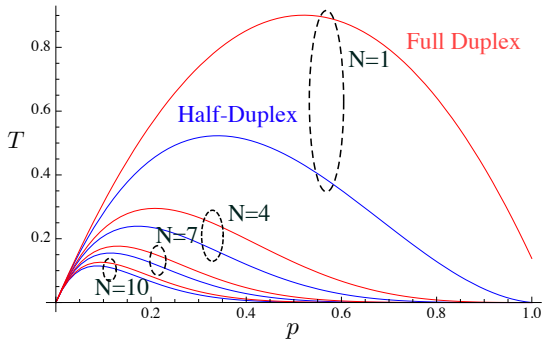

Fig. 4: Channel achievable transmission rate T in bits/s/Hz as a function of the number of nodes N connected to the hub. $\theta = 10$dB, $\sigma = 4dB$, links SINR=10dB.

B. Mesh Topologies

Referring back to Fig. 1, it can be seen that a BAN build using a mesh topology can be approximated as a cylindrical surface of radius r and height $2h$ deployed on a human torso. Without any loss of generality, the center of the reference axes can be located on the receiver node. Therefore, as shown in Fig. 5, the body area network can be modeled as a finite, rectangular area of width $2\pi r$ and height $2h$. For a regular deployment of N nodes on the surface $A = 2\pi r.2h$, the inter-nodes distance is $\delta = \sqrt{2\pi r.2h/N}$. For instance, let us fix: $2\pi r = 1$ m and $2h = 0.5$ m, so that $\delta = 1/\sqrt{2N}$.

It is interesting to note that the term $10^{\gamma(d_0-d_i)}$ is virtually insensitive to an increase in the amount of nodes deployed on the body surface. Indeed, if the amount of nodes is multiplied by a factor α, the transmission distances are divided accordingly, so that the term becomes $10^{\gamma(d_0-d_i)/\alpha}$. Since γ is large (authors in [10] report $\gamma = 126$dB/m) and distances are limited, the value of α has a small impact on the exponent expression. This can also be interpreted as the fact that only the direct neighbors do interfere on communications: these are limited by interference from *dominant nodes*.

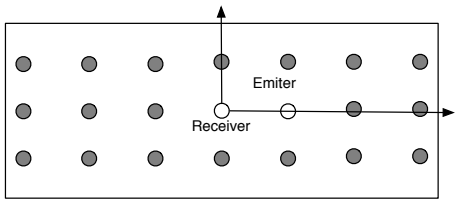

Fig. 5: Schematic representation of a regular deployment of sensors.

In Fig. 6, the throughput is plotted in a scenario similar to Fig. 5 and with respect to the transmission distance. This distance is expressed in terms of nodes hopped over, i.e., $d_0 = n\delta$. More precisely, the transmission goes from $n = 1$ (direct transmission to the closest neighbor) to $n = 4$ (transmission four hops away).

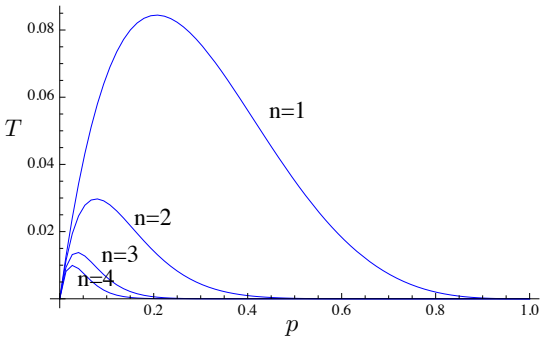

Fig. 6: Channel achievable transmission rate T in bits/s/Hz as a function of the hop distance (expressed in number of intermediary hop nodes n). $\theta = 10$dB, $\sigma = 4$dB, links SINR=10dB.

It can be seen that, when the sensing rate is low ($p \ll 1$), long-range transmissions are to be preferred (for delay and energy considerations). On the other hand, when $p \geq 0.05$, short-range communications and multi-hopping are more suitable.

C. Sustainable Number of Hops

In the context of multi-hop communications, each transmission takes place on a route in which a certain amount of intermediary nodes act as relays. The maximum sustainable number of nodes (that is, the route length) is a critical parameter since it quantifies the effective distance that can be covered and is an indicator of the connectivity of whole the network [13]. It depends on the acceptable packet loss, link interference, and topology among others.

In a conservative scenario, each node stores and forwards every packet it receives, without any consideration for re-transmissions. This case, though pessimistic, corresponds to UDP-style connections and allows to derive the lower of bound of the network performance. Since all links are considered equals, the *route* probability of success is

$$\mathcal{P}_{\mathrm{s}}^{\mathrm{route}} = \prod_{i=1}^{n_{\mathrm{hops}}} \mathcal{P}_{\mathrm{s}}^{(i)} = \left(\mathcal{P}_{\mathrm{s}}\right)^{n_{\mathrm{hops}}}.$$

Therefore, the maximum sustainable amount of hops for an acceptable final transmission success equal to $\mathcal{P}_{\text{s}}^{\text{th}}$ is

$$n_{\text{hops}} = \left\lfloor \frac{\log\left(\mathcal{P}_{\text{s}}^{\text{th}}\right)}{\log\left(\mathcal{P}_{\text{s}}\right)} \right\rfloor$$

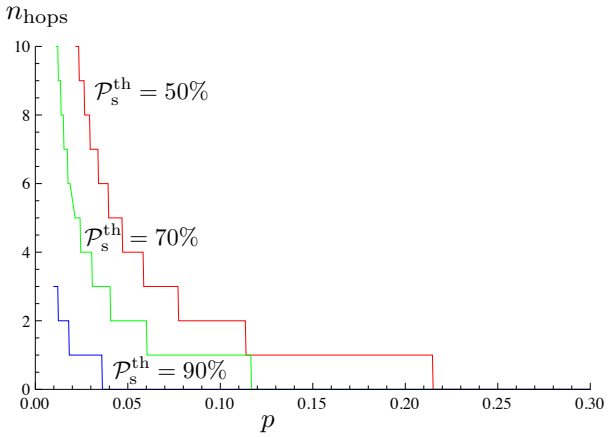

Fig. 7: Maximum sustainable number of hops with regular topology and for different values of the acceptable route probability of sucess. $\theta = 10$dB, $\sigma = 4dB$.

In Fig. 7, the maximum number of sustainable hops is presented for various values of the minimal route probability of success $\mathcal{P}_{\text{s}}^{\text{th}}$. It can be observed that (without any form of transmission control), highly-reliable routes can only be achieved at very low transmission rates. Also, most routes exhibit a limited amount of possible hops but these values should be sufficient enough to achieve full connectivity in the specific context of body area networks.

V. Conclusions

In this paper, we have derived a closed-form expression for the link probability of success in interference-limited BANs subject to large-scale fading. In the presence of a centralized network topology, it has been shown that the duplex capability of the nodes does not play a critical role, especially in the presence of limited sensing rates. It has been shown that a maximum achievable transmission rate exists and depends on the amount of deployed nodes. Beyond this maximum, the interference makes the achievable transmission rate decrease.

For BANs with a mesh topology, the transmission strategy depends on the traffic profile. More precisely: when the transmission probability of each node is limited (passive monitoring of a patient or deep sleep of the nodes), long-range transmissions can be used in order to save energy and avoid multiple relays. On the other hand, when the sensors have a substantial amount activity, the performance decreases exponentially with the number of hops. Shortest possible hop strategy should be used but it comes at the cost of numerous relaying. However, even though the maximum sustainable number of hops is small, it is still suitable for BAN-based applications. Finally, it has also been observed that it is extremely difficult to reach a security level of 90% without a transmission control protocol.

Appendix

The modeling of slow-scale fading as a Log-normal distribution (that is, a zero-mean Gaussian in dB scale) raises mathematical difficulties, as shown in (4). The complementary cdf. of the zero-mean Log-normal distribution is

$$\zeta(z;\sigma) = \frac{1}{2} + \frac{1}{2}\text{erf}\left(\frac{-10\log_{10} z}{\sigma\sqrt{2}}\right) \tag{8}$$

This function is plotted on Fig. 8 for $\sigma \in [4, 16]$. It can be observed that (i) $\zeta(z)$ saturates for $z \to \infty$ and (ii) it has the shape of a decreasing exponential function.

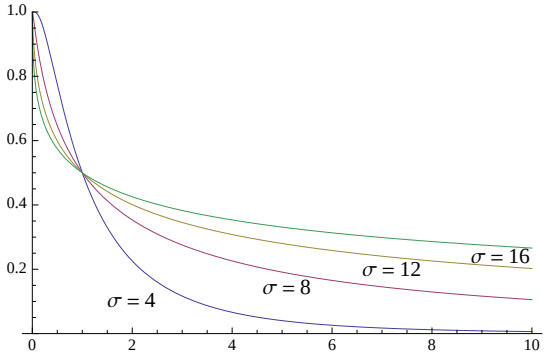

Fig. 8: $The function \zeta(z)$ for $\sigma = 4 - 16$dB

Indeed, the erf(.) function is known to have the following approximations:

$$\begin{aligned}
\text{erf}(x) &\approx 1 - \frac{e^{-x}}{x\sqrt{\pi}} \\
&\approx \frac{1}{x\sqrt{2\pi}}\left(1 - \frac{1}{x^2}\right)e^{-x^2} \\
&\approx \sqrt{1 - \exp\left(-\frac{2x}{\sqrt{\pi}}\right)}\text{, etc.}
\end{aligned}$$

The $\zeta(.)$ function can therefore be approximated with a linear combination of negative exponential function, as in Prony's approximation [14]:

$$\zeta(z) = \sum_{j}^{\infty} c_j \exp(-a_j z) \approx \sum_{j}^{n} c_j \exp(-a_j z)$$

where the coefficients $\{c_j\}_{j=1\ldots n}$, $\{-a_j\}_{j=1\ldots n}$ are determined in a least square sense by means of $q \geq 2n$ known points of the $\zeta(.)$ function. A Levenberg-Marquardt algorithm [15], [16] was used to determine the coefficients $\{c_j\}$ and $\{a_j\}$ for different values of σ and $q = 10000$ points over the interval $z \in [0, 1000]$. The corresponding values are reported in Table I along with the corresponding residual sum of squares.

TABLE I: Prony coefficients for the approximation of $\zeta(.)$

	c_1	a_1	c_2	a_2	c_3	a_3	residual
$\sigma = 4$	0.49	0.75	0.49	0.75	0.03	0.16	$4.68\,10^{-5}$
$\sigma = 6$	0.38	0.31	0.56	1.21	0.06	0.07	$4.23\,10^{-6}$
$\sigma = 8$	0.59	1.32	0.34	0.18	0.06	0.02	$1.04\,10^{-4}$
$\sigma = 10$	0.29	0.09	0.65	1.17	0.05	0.01	$7.53\,10^{-4}$
$\sigma = 12$	0.04	0	0.24	0.04	0.70	0.93	$3.52\,10^{-3}$
$\sigma = 14$	0.20	0.01	0.03	0	0.72	0.64	$1.03\,10^{-2}$
$\sigma = 16$	0.18	0.01	0.70	0.49	0.04	0	$1.67\,10^{-2}$

REFERENCES

[1] E. Reusens, W. Joseph, G. Vermeeren, and L. Martens, "On-body measurements and characterization of wireless communication channel for arm and torso of human," *4th international workshop on wearable and implantable body sensor networks (BSN 2007)*, vol. 13, pp. 264–269, 2007.

[2] J. M. Choi, H.-J. Kang, and Y.-S. Choi, "A study on the wireless body area network applications and channel models," in *FGCN '08: Proceedings of the 2008 Second International Conference on Future Generation Communication and Networking*. Washington, DC, USA: IEEE Computer Society, 2008, pp. 263–266.

[3] N. Katayama, K. Takizawa, T. Aoyagi, J.-I. Takada, H.-B. Li, and R. Kohno, "Channel model on various frequency bands for wearable body area network," *IEICE Transactions on Communications*, vol. E92.B, no. 2, pp. 418–424, 2009.

[4] A. Fort, C. Desset, P. De Doncker, P. Wambacq, and L. Van Biesen, "An ultra-wideband body area propagation channel model-from statistics to implementation," *IEEE Transactions on Microwave Theory and Techniques*, vol. 54, no. 4, pp. 1820– 1826, 2006.

[5] H. Sawada, J. Takada, S. Choi, K. Yazdandoost, and R. Kohno, "Review of body area network channel model," in *Proc. IEICE Gen. Conf.*, 2007.

[6] J. Ryckaert, P. D. Doncker, R. Meys, A. de Le Hoye, and S. Donnay, "Channel model for wireless communication around human body," *Electron. Lett.,*, vol. 40, no. 9, pp. 543–544, 2004.

[7] P. Gupta and P. R. Kumar, "The capacity of wireless networks," vol. 46, no. 2, pp. 388–404, Mar. 2000.

[8] X. Liu and M. Haenggi, "Throughput analysis of fading sensor networks with regular and random topologies," *EURASIP J. Wirel. Commun. Netw.*, vol. 2005, no. 4, pp. 554–564, 2005.

[9] J. ichi Takada, T. Aoyagi, K. Takizawa, N. Katayama, H. Sawada, T. Kobayashi, K. Y. Yazdandoost, H. bang Li, , and R. Kohno, "Static propagation and channel models in body area,," in *COST 2100 6th Management Committee Meeting, TD(08)639*, 2008.

[10] S. van Roy, C. Oestges, F. Horlin, and P. De Doncker, "Propagation modeling for uwb body area networks: Power decay and multi-sensor correlations," in *IEEE 10th International Symposium on Spread Spectrum Techniques and Application*, 2008, pp. 649–653.

[11] D. Bertsekas and R. Gallager, *Data Networks*, Prentice-Hall, Ed., 1991.

[12] S. Ahmed and M. S. Alam, "Performance evaluation of important ad hoc network protocols," *EURASIP Journal on Wireless Communications and Networking*, vol. 2006, pp. Article ID 78 645, 11 pages, 2006.

[13] O. K. Tonguz and G. Ferrari, *Ad Hoc Wireless Networks: A Communication-Theoretic Perspective*. Chichester, UK: John Wiley and Sons, March 2006.

[14] Baron G. de Prony, "Essai expérimental et analytique sur les lois de la dilatabilité des fluides élastique et sur celles de la force expansive de la vapeur de l'eau et de la vapeur de l'alkool, à différentes températures," *Journal de l'École Polytechnique*, vol. 1, no. 2, pp. 24–76, 1795.

[15] K. Levenberg, "A method for the solution of certain non-linear problems in least squares," *The Quarterly of Applied Mathematics*, vol. 2, pp. 164–168, 1944.

[16] D. Marquardt, "An algorithm for least-squares estimation of nonlinear parameters," *SIAM Journal on Applied Mathematics*, vol. 11, pp. 431–44, 1963.